This paper is a postprint of a paper published in Springer Nature link-Journal of Electrical Engineering & Technology (2023) 18, 3179–3190

https://doi.org/10.1007/s42835-023-01413-2 and is subject to The Korean Institute of Electrical Engineers 2023

Real-Time Power Quality Event Monitoring System Using Digital Signal Processor for Smart Metering Applications

Naveen Kumar Buduru[1] · **Srinivas Bhaskar Karanki**[1]

Abstract

Due to the enormous increase of domestic and industrial loads in the smart grid infrastructure, the power quality issues are very frequent. It is essential to monitor the quality of power being supplied to customers. To identify the quality of the power effectively at various locations, a simple solution is needed that limits the usage of computing resources and can also be deployed in remote location. This paper proposes a low-computational, automatic, real-time PQ monitoring system based on the Hilbert transform (HT), fuzzy logic and threshold based classifiers. The major contribution of the proposed method is based on sample-to-sample process that can detect the events timely, unlike a ten-cycle window-based methods. Six power quality disturbances are synthetically generated using mathematical model as per the IEEE 1159–1195 standard. The methodology utilizes HT for the extraction of the instantaneous amplitude from the filtered signal. Thereby, the essential features are extracted and fed to classifier to improve the recognition capability. The robustness of the proposed algorithm is verified in a MATLAB environment with different signal-to-noise ratios. An experimental prototype has also been developed using TMS320F28379D Launchpad to validate the proposed PQ monitoring algorithm using both synthetic and real-time PQ signals. The real-time implementation demonstrates that the proposed PQ sensing hardware and PQ disturbance analysis software are effective, fast, and accurate.

Keywords Advanced metering infrastructure · Hilbert transform · Fuzzy logic · Power quality monitoring · Power quality disturbance classification · Smart grid

1 Introduction

In a smart grid environment, power quality monitoring has become a critical task due to the increasing number of wide categories of disturbances. These disturbances impacts acutely a lot of domestic loads, power systems that are tightly coupled with power semiconductor devices, and many critical loads [1, 2]. Power quality disturbance (PQD) refers to deviations in either frequency or magnitude from the ideal waveform with rated parameters [2]. According to IEEE 1159–1995 [2], power quality disturbances are classified harmonics, oscillatory transients, normal, sag, swell, and interruption. Because of the numerous sources of PQ disturbances, power supply quality has become a major concern among electric power suppliers. As a result, the quality of power delivered must be continuously monitored for both electric utilities and customers. This helps in avoiding the significant financial losses and equipment damage. Thus, detection and classification of PQ disturbances are highly desirable for improving the quality of service and enhancing the productivity of the systems [3–6].

Various PQD detection and classification methods were proposed using signal processing techniques. In these methods, feature extraction is a crucial task in classifying the events correctly with high accuracy. In order to obtain more discriminant features, advanced signal processing techniques have been developed. It includes combination of time–frequency tools, adaptive mode decomposition, and deep learning techniques. Recently, the analysis of PQ events using time–frequency tools such as short-time Fourier transform (STFT), wavelet transform (WT), and s-transform (ST) have gained popularity. STFT utilizes a shifted window-based Fourier transform to obtain time and frequency information

✉ Naveen Kumar Buduru
bnk11@iitbbs.ac.in

Srinivas Bhaskar Karanki
skaranki@iitbbs.ac.in

[1] School of Electrical Sciences, IIT Bhubaneswar, Bhubaneswar, India

of the disturbance [7, 8]. Because of fixed window, the time resolution and frequency resolution are poor while analyzing PQ events. To overcome the shortcomings, a wavelet transform has been developed with a scaled window structure to obtain time–frequency information [9–11]. However, it degrades phase information in noisy conditions. The S-transform uses a scalable localized moving Gaussian window that can embed the features of both WT and STFT [12–14]. It preserves localized frequency information more precisely than WT and STFT due to variable window size. It is varied according to the frequency components of the signal. Even though it provides accurate time–frequency information, due to high computational burden, the method is not suitable for real-time PQ event monitoring.

On the other hand, the PQ methodologies developed based on adaptive decomposition algorithms have also gained research attention. Empirical mode decomposition (EMD) is a method for analyzing non-linear and non-stationary signals [15]. It decomposes a non-stationary signal into multiple stationary signals through a sifting process. It's hardware implementation requires low computational resources. However, it still comprises of some issues inherently such as mode mixing leads to erroneous modes. Further, different variants of the EMD are proposed to overcome the problems in original EMD [16]. But it suffers with huge computational complexity. Hilbert Huang transform (HHT) based PQ methodologies are also investigated. It comprises basic building blocks of EMD, and Hilbert transform for extracting time and instantaneous frequency-based features [17]. In [18], the authors developed a novel non-recursive framework based on variational mode decomposition for the PQ disturbance detection. It decomposes a complex nonstationary signal into band-limited intrinsic mode functions. It utilizes a basic building block of wiener filter, Hilbert transform, and frequency translation. It decomposes the modes precisely than EMD and HHT. In contrast, the VMD requires two parameters such as bandwidth and number of modes priorly. Finally, each PQD detection and classification methods have its own advantages and limitations with respect to the specific application scenarios.

1.1 Related Works

Recent research into smart grid PQ monitoring has been focused on developing methods for detecting and identifying PQ and getting PQ indices from the smart meters. However, most commercially available smart meters are developed for energy monitoring purposes [19]. Even though the smart grid environment is expanding, PQ detection algorithms are missing on the smart meter [20]. In [8], the authors proposed a framework for power quality disturbances using different deep learning techniques with the STFT. In this framework, seven power quality disturbances are detected using LSTM, CNN, CNN-LSTM. The authors reported results in the PC environment with the validation accuracy of 79.14% for LSTM, 84.58% for CNN, and 84.76% for CNN-LSTM, 83.66% for the CNN-LSTM with tuned hyperparameters. In [12], an online PQ event detection and identification system has been proposed based on the S-transform and ANN-based classifier. Furthermore, a hardware setup has been used for collecting real PQ data using NI-cDAQ and classifying PQ disturbances on the PC environment. In [16], Liu et al. proposed an ensemble empirical mode decomposition and rank wavelet support vector machine based classification method for multiple PQ events on the real-time digital simulator (RTDS) platform. In [17], Sahani et al. proposed the Hilbert Huang transform and weighted bi-directional extreme learning machine classification system. It uses the four simple features for identifying the PQ disturbances. Further, a hardware setup is developed for real-time power quality monitoring using TMS320C6713. However, by using these algorithms on the smart meter, the financial burden increases for PQ monitoring at various locations. In [21], the authors proposed two parallel stage VMD for identifying PQ disturbances with a decision tree. The proposed method uses four simple features for classifying 14 PQ disturbances and obtains a classification accuracy of 99.46%. For a PQ signal duration of 200 ms, the method reported a computational time of 180 ms. The authors demonstrated a hardware setup for detecting real PQ signals based on RTDS that utilizes a parallel processing block which is not available in low-end devices. In [22], nine efficient features are extracted from the two-level decomposition of a discrete wavelet transform. The methodology is combined with support vector machine to identify the four PQ disturbances in the PQ signal. It is developed for smart meter applications and have the following features: lightweight, fast, and low-computational resources. In addition, it achieves an acceptable classification accuracy of 97%. However, the author did not report any hardware setup. To meet real-time constraint, the higher-end signal processing boards are required which increase the financial burden. Although, all these techniques are well suited for offline purposes and developed in the personal computer (PC) environment.

1.2 Research Gap

An extensive research is conducted on the recent PQD detection and classification methods. However, the existing works have research gaps as presented here. Firstly, most of the methods are employed to detect more number of PQ disturbances. However, most of the authors have not considered the real-time feasibility of the proposed framework. Secondly, the implementations of the existing frameworks require high-end signal processing boards such as RTDS, TMS320C6713DSP, etc. and their performance was not studied on a low-resource computing platforms. It is the most important factor in reducing the overall cost of smart metering. Thirdly, most of the frameworks uses 10 cycles window information for identifying PQ disturbances that limits the timely PQ events detection. Finally, since the computational resources are limited in low-cost DSP boards, investigating light-weight signal processing and classification techniques is highly demanded ensuring accurate and reliable detection of primary PQ disturbances. Thus, developing affordable smart metering with PQ monitoring has become more important to provide feasible PQ event information for consumers.

1.3 Major Contributions

The goal of this paper is to develop a real-time signal processing algorithm with lower complexity for PQ event monitoring in a smart meter application. In this aspect, a new PQ methodology has been developed with Hilbert transform method that uses a sample-to-sample process for the disturbance detection. The proposed framework consists of digital filtering, Hilbert transform, feature extraction, fuzzy classifier, and threshold-based classifier. The methodology can detect and classify the PQ events into normal, swell, sag, interruption, harmonics, and oscillatory transients. The proposed PQ framework is implemented on the TMS320F28379D Launchpad computing platform to demonstrate the real-time feasibility of the proposed PQ monitoring system along with various simulation studies in MATLAB. The real-time system is built around the Launchpad board that is interfaced with PQ data acquisition hardware and a visualization interface on a PC to display power line waveform and PQD information. The experimental results demonstrate that the proposed real-time PQ monitoring system is suitable for industrial and domestic smart metering with continuous PQ event monitoring for timely detection of power quality disturbances. The major contribution of the presented work includes developing a lightweight, sample-to-sample, and real-time PQ event monitoring system and designing the low-cost hardware setup for the PQ event detection. The main features of the proposed PQD algorithm are as follows:

1. Proposed a lightweight signal processing technique for detecting and classifying power quality events using Hilbert transform.
2. This approach adequately depicts the nature of six PQ events with four simple and essential features.
3. The suggested method can accurately recognize and categorize PQ events in a noisy and noise-free environment.
4. This paper demonstrates the implementation and real-time feasibility of the proposed technique on a hardware platform. It compares with a standard fluke power analyzer to show the performance superiority in terms of the magnitude and duration of the events.

The rest of this paper is organized as follows: Sect. 2 describes the typical behavior of PQ events, the generation of power quality disturbances, and proposes a Hilbert transform based algorithm for the detection and classification of PQ events. Section 3 presents the integration of hardware components and software implementation of the proposed Hilbert-based methodology for real-time monitoring. In Sect. 4, various results are presented to demonstrate the efficacy of the proposed system for the detection and classification of PQ disturbances. The pros and cons of the proposed PQ methodology discussed in Sect. 5. Finally, the conclusions are drawn in Sect. 6.

2 Proposed Real-Time Power Quality Event Monitoring

2.1 PQD Database Creation

The availability of real PQ signals is limited because the collection of data requires a long monitoring time as well as there is ambiguity in the occurrence of PQ events at different locations. So, the PQ database has been generated using mathematical models and simulated in the MATLAB platform. These numerical models are created according to the IEEE 1159–1995 standard, and they closely depict the real PQ disturbances. The typical behavior of each type of disturbance can be known with the duration and magnitude of the disturbance signal shown in Table 1. The following signals are considered for further analysis in this paper, as shown in Table 2.

Table 1 Typical characteristics of the PQ disturbances

Type of PQ disturbance	Typical duration	Typical voltage magnitude
Sag	>0.5 cycles	0.1–0.9 pu
Swell	>0.5 cycles	1.1–1.8 pu
Interruption	>0.5 cycles	<0.1 pu
Harmonics	>50 ms	0.0–0.2 pu
Oscillatory transients	$5<t<50$ ms	0–8 pu

Table 2 Summarizes the mathematical models and their parameters used for generating different kinds of PQD signals

Type of PQ disturbance	Mathematical model	Parameters
Normal (CL1)	$Asin(wt)$	$w = 2\pi f, f = 50, A = 1, T = \frac{1}{f}$
Sag (CL2)	$A\left(1 - \alpha\left[u\left(t - t_1\right) - u\left(t - t_2\right)\right]\right) \sin(\omega t)$	$0.1 \le \alpha \le 0.9$ $T < t_2 - t_1 < 9T$
Swell (CL3)	$A\left(1 + \alpha\left[u\left(t - t_1\right) - u\left(t - t_2\right)\right]\right) \sin(\omega t)$	$0.1 \le \alpha \le 0.9$ $T < t_2 - t_1 < 9T$
Interruptions (CL4)	$A\left(1 - \alpha\left[u\left(t - t_1\right) - u\left(t - t_2\right)\right]\right) \sin(\omega t)$	$0.9 \le \alpha \le 1.0$ $T < t_2 - t_1 < 9T$
Harmonics (CL5)	$A \sin(\omega t) + \sum_{k=3}^{7} \beta_k \sin(kwt)$	$0.05 < \beta_k < 0.15$
Oscillatory transients (CL6)	$Asin(wt) + \alpha e^{-(t-t_1)/\tau} \sin\left(\omega_n\left(t - t_1\right)\right)\left[u\left(t - t_2\right) - u\left(t - t_1\right)\right]$	$300 \le f_n \le 900$, $8ms \le \tau \le 40ms$, $0.1 \le \alpha \le 0.8$, $0.5T \le t_2 - t_1 \le 3T$

2.2 PQD Detection and Classification Methodology

The proposed power quality disturbance detection and classification algorithm shown in Table 3 and it consists of the following three major stages:

- **Digital Filtering for Waveform and Transient Events:**

To detect PQ disturbances, lowpass (LPF) and high-pass filter (HPF) based filtering frameworks are employed. HPF is used to separate transients and harmonics from other waveform fluctuations, while LPF is used to capture fundamental signal variations.

- **Analytical Waveform and Feature Extraction:**

The instantaneous amplitude features of the filtered signal are extracted from the HT. The extracted envelope feature is used at the classification stage.

- **Classifier:**

The fuzzy rules are constructed for detecting and classifying PQ events such as swell, normal, sag, and interruption. The simple threshold-based classifier is used for classifying oscillatory transients and harmonics based on the time duration of the event.

2.2.1 Digital Filtering for Waveform and Transient Events

A number of methods have been reported based on various signal decomposition techniques to distinguish the transient events from the other waveform magnitude and frequency distortions. However, this paper presents a traditional filtering structure used to obtain the waveform distortions and transient events. The third-order Butterworth low-pass filter is designed with a higher cut-off frequency of 100 Hz to extract waveform variations and suppress high-frequency components. The IIR based low-pass filter is chosen instead of fir based low-pass filter due to its better response at the smallest order. Also, it provides a minimal phase delay which reduces the detection time of the proposed framework. The order of the IIR low-pass filter is chosen by conducting repetitive experiments that minimizes phase delay and should not affect the filter response. Similarly, the fifth order Butterwort high-pass filter is designed with the cut-off frequency of 100 Hz. The filter order is chosen such that it completely removes the fundamental 50-Hz component.

2.2.2 Analytical Waveform and Envelope Extraction

For extracting the envelope of the PQ disturbance signal, HT is used in this study. The envelope is obtained from the analytical signal, which has both real and imaginary parts of the signal. The imaginary part, which is a 90 ° phase-shifted version of the applied signal, is obtained from the HT. The HT of a continuous signal $x(t)$ is computed using (1).

$$x_{HT}(t) = \frac{1}{\pi} \int_{-\infty}^{\infty} \frac{x(\tau)}{t - \tau} d\tau \quad (1)$$

The analytical signal $Z(t)$ obtained from the Hilbert transform is shown in (2)

$$Z(t) = x(t) + jx_{HT}(t) = E(t)e^{\theta(t)} \quad (2)$$

where $E(t)$ indicates the envelope of the signal

$$E(t) = \left(x(t) + x_{HT}(t)\right)^{1/2}$$

and $\theta(t)$ gives the instantaneous phase of the signal.

Table 3 Proposed algorithm for detection of power quality events using Hilbert transform

[CL1, CL2, CL3, CL4, CL5, CL6] =Disturbance_Detection ($x[n]$)
Input: $x[n]$ = PQ Signal
F_s = Sampling frequency
Step1: The signal applied to a third order IIR LPF and fifth order IIR HPF designed with a cut-off frequency of 100 Hz.
x_l :=Voltage signal having a low frequency information
x_h :=Voltage signal having a high frequency information
Step2: Compute the Hilbert transform of the low-pass filter response.
Step3: The analytical signal obtains from
$z_l(t) = x_l(t) + j\, x_{lHT}(t)$
Step4: The envelope of a low-pass filtered output obtains from an analytical signal.
$E_l = \sqrt{x_l(t)^2 + x_{lHT}(t)^2}$
Step5: The moving average filter designed with following specifications to remove ripples present in the envelope
$NL = floor(0.01 * Fs);\ WL = rectwin(NL)/NL;$
$Y_{lM} = filter(WL, 1, E_l);$
Step6: The filter response passed through the Derivative filter.
$d' = Y_{lM}[n] - Y_{lM}[n-1];$
$x_{zh} = 0$ if $d' \geq 0.0001$ or $d' \leq -0.0001$
$x_{zh} = x_h$ otherwise
Step7: The magnitude of the derivative filter has satisfied certain threshold then the zero mapping unit forces the high-pass filter response to zero.
Step8: Compute the Hilbert transform of high-pass filter output using (1)
Step9: The envelope of a high-pass filtered output obtains from analytical signal.
$E_{zh} = \sqrt{x_h(t)^2 + x_{zhHT}(t)^2}$
Step10: The envelope $E_h(n)$ is given to moving average filter
$NH = floor(0.02 * Fs);\ WH = rectwin(NH)/NH;$
$Y_{hM} = filter(WH, 1, E_{zh});$
Step11: The Y_{hM} has given to fixed threshold to detect the on-time of the event
Step12: The derivative filter and moving average filter output given rule-based fuzzy. For developing code, the following commands used in MATLAB.
$fis = readfis('tipper');$
type the rules using $ruleedit(fis);$
classify the events such as CL1, CL2, CL3, and CL4 using $evalfis(input1, input2);$
Step13: The Y_{hM} has given to fixed threshold to detect CL5 and CL6 based on the time duration of the event

$$\theta(t) = \tan^{-1}\left(\frac{x_{HT}(t)}{x(t)}\right)$$

The proposed method is designed to detect, locate, and classify PQ disturbances based on the instantaneous amplitude extracted from the PQ signal. The HT is computed by convolving the filtered signal with $1/(\pi t)$. The order is chosen 0.02 times sampling frequency such that it reduces the ripples present in the envelope response (E_l). Even though, ripples still exist in the envelope that causes false classification, and impacts on-duration of the PQ events. Therefore, the moving average filter is used to smooth out the ripples present in the envelope and it is fixed as 0.01 times the sampling frequency. To determine the starting and ending points of the PQ event, the derivative filter response is computed on the smoothed instantaneous amplitude. Finally, the derivative filter response (d') and moving average filter responses (Y_{lm}) are given to identify the fuzzy classifier.

Similarly, the high-pass filtered response (x_h) consists of oscillatory, transient components, and other high frequency component due to phase jumps. These phase jumps occur during the transition of sag, swell, and interruption events. To tackle this issue, a non-linear zero-mapping filter (x_{zh}) has been designed. It utilizes a derivative filter response (d') in the design process. The magnitude of a derivative filter satisfies a predefined threshold, i.e. either higher than 0.001 or less than -0.001. Then, the zero-mapping unit maps the high-pass filtered signal (x_h) to zero. The thresholds are chosen for the minimum magnitudes of the derivative filter during sag. However, the high frequency component still exists in the envelope response (E_{zh}) It is further reduced using moving average filter and its order chosen 0.02 times sampling frequency. Finally, the response is given to threshold unit to classify the PQ events.

2.2.3 Classifier

The fuzzy logic framework is widely used for solving physical problems. In general, these problems are either do not govern a proper mathematical model or very complicated to encode data. Therefore, a set of rules is framed based on human ability and includes knowledge-based information about the system. The superiority of fuzzy logic (FL) systems strongly depends on the knowledge of human experts for the specified application; hence, it is only as good as the legitimacy of the rules. In this stage, the FL framework is implemented for classifying the PQ events based on voltage variations present in the PQ signal. With two inputs, one output, and 12 rules, a Mamdani type fuzzy inference system is created. For the fuzzification process, one input signal is considered from the instantaneous amplitude (IA) of the signal, while the other is taken from its derivative amplitude (DA). The envelope signal amplitude has been categorized into four trapezoids, indicated as follows: large amplitude (LA), normal amplitude (NA), small amplitude (SA), and very small amplitude (VSA). The boundaries of the envelope signal is considered as per the IEEE 1159 standard. In the same way, the derivative amplitude is divided into three trapezoids, each with its own label: positive derivative (PD), zero derivative (ZD), and negative derivative (ND). The boundaries of the derivative filter are framed by considering all the possibilities of the derivative amplitudes for the PQ disturbances. The fuzzy response (FR) has been divided into four trapezoids: swell, normal, sag, and interruption. The membership function for the IA, DA, and FR have shown in Fig. 1. The rules are considered as follows:

1. If (IA is VSA) and (DA is ND), then (FR is interruption).
2. If (IA is VSA) and (DA is ZD), then (FR is interruption).
3. If (IA is VSA) and (DA is PD), then (FR is sag).
4. If (IA is SA) and (DA is ND), then (FR is sag).
5. If (IA is SA) and (DA is ZD), then (FR is sag).
6. If (IA is SA) and (DA is PD), then (FR is normal).
7. If (IA is NA) and (DA is ND), then (FR is normal).
8. If (IA is NA) and (DA is ZD), then (FR is normal).
9. If (IA is NA) and (DA is PD), then (FR is normal).
10. If (IA is LA) and (DA is ND), then (FR is normal).
11. If (IA is LA) and (DA is ZD), then (FR is swell).
12. If (IA is LA) and (DA is PD), then (FR is swell).

To detect harmonics and oscillatory transients, a threshold-based classifier has been designed. In this method, the fixed threshold has been set as the maximum magnitude response of the moving average filter obtained in the swell case. It tracks the on-duration of these events. The duration of the event is determined as the time during which the envelope continuously exceeds the magnitude threshold level.

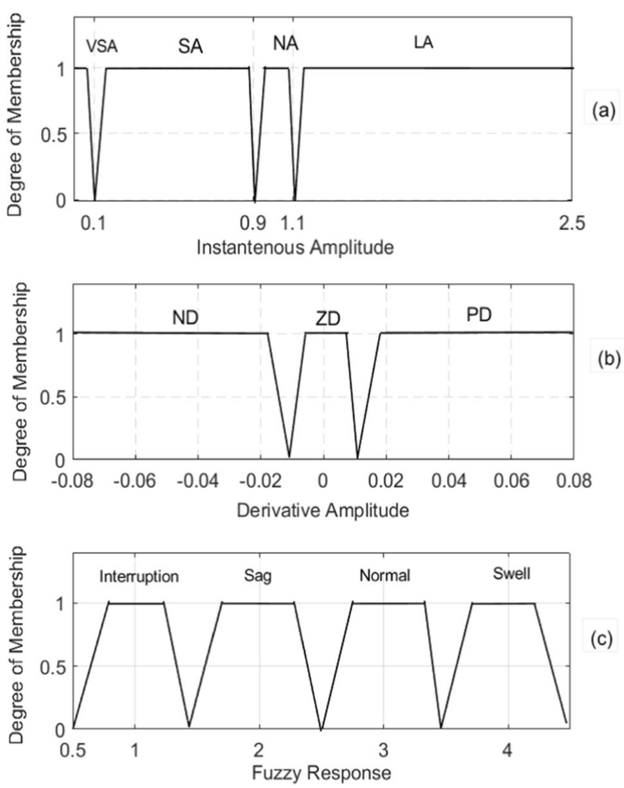

Fig. 1 Membership functions for the **a** Instantaneous amplitude, **b** Derivative, and **c** output

Finally, the duration of an event is used for identifying the oscillatory transients (5 ms < DT < 50 ms) and the harmonics (DT > 50 ms) according to the IEEE 1159–1195 standard.

3 Real-Time Implementation

This section presents the development of a hardware prototype with the proposed PQD event monitoring algorithm for real-time monitoring of PQ disturbances. The significant components are the signal conditioning circuit and the DSP signal processor board.

The signal processor board used in this work is the TMS320F28379D Launchpad. The Launchpad has two 32-bit floating-point processors, and each processor runs with a 200 MHz clock. The selection of this board is made due to its internal subsystems such as the Floating-point unit, Trigonometric math unit, and Viterbi/Complex math unit. These subsystems are greatly enhancing the performance of the DSP board in terms of handling much more computations. This board is widely used in signal processing applications. Some of the specifications of the Launchpad include 24 enhanced pulse width modulation (EPWM) channels, three 12-bit digital-to-analog (DAC) modules, and four analog-to-digital (ADC) modules.

3.1 Hardware Setup

The first stage of hardware development includes the generation of real-time PQ disturbances. In this paper, the disturbances are generated using a programmable power supply (PPS). The disturbances are generated from the PPS such as swell, sag, and interruption with the following specifications: time of event generation and amplitude. Similarly, harmonics and oscillatory transients are generated with their corresponding specifications. A single-phase signal with disturbances generated from the PPS is given to the sensor and signal conditioning circuit. The sensor board contains a voltage sensor and a current sensor. These sensors are used to sense the voltage and current parameters of the power supply to scale down the required suitable voltage for the operation of the signal processing board. For example, 230 V sensed by sensor board is converted into 5 V. The sensor board is developed using Hall effect transducers to provide the isolation between power level and signal level circuits. The output of the sensor board is given to the signal conditioning board for further reducing the signal level to 0–3 V. It is built on the TL064 IC that has four operational amplifiers. Each amplifier is dedicated to a particular operation: the first operational amplifier is used to construct a buffer circuit that provides high impedance. Therefore, it reduces overloading effects. The attenuator is used in the next stage to further reduce the signal level. The output of the attenuator is given to a 1.5 V DC level shifter to read the bipolar signal in the analog channel using the single-ended ADC. Otherwise, the negative portion of the signal is represented by zero volts. The final op-amp is used for a precision circuit with a diode in the feedback loop to remove the excess negative voltage, which would have caused dam-age to the processor. The output is collected across the Zener diode, which limits the signal range to a maximum of 3.3 V. The TMS320F28379D board is connected to a laptop using USB cable and the algorithm is programmed on the board using CCS in the laptop. To read the output signal from the sensor, the signal conditioning board is connected to pin 30 and pin 22 (ground) of the J3 booster pack. After processing the data by the TMS320F28379D board, results are displayed using a digital storage oscilloscope (DSO). To monitor results on the DSO, analog data available at pin 30 and pin 22 (GND) of the J7 booster pack is connected to DSO probes. Figure 2 shows the laboratory-based hardware prototype which was developed for monitoring real-time PQ disturbances.

3.2 Development of Algorithm

The proposed algorithm is developed in Code Composer Studio (CCS). It is an integrated development environment that has a set of tools used to build and debug embedded applications. It supports both C and assembly language for the software development of TI's family. The algorithm is programmed in C language and the code is dumped in the TMS320F28379D Launchpad using CCS. Figure 3 depicts the code flow of the proposed algorithm. It has two routines: one main routine and the second interrupt service routine. The main routine has the initialization of major DSP modules such as ADC, DAC, system clocks, and pulse width modulations. The interrupt service routine consists of a signal processing algorithm and classifier. It reads the sample-by-sample data for identifying the PQ events detection and classification. For the data acquisition, the Launchpad of the ADC module is configured with several parameters for digitizing the PQ signal: resolution, signal mode, end of conversion (EOC), the start of conversion (SOC), and ADC clock. A 12-bit single-ended ADC is used for acquiring the digital signal with a resolution of 732.6 μV. The sampling frequency of ADC is set to 3.2 kHz to collect the sampled signals. The EPWM1 module is configured to provide the sampling frequency to trigger the ADC module on a period match using the SOCA trigger. The program performs the conversion on the ADC channel A0 and the digitized data is available at the ADCRESULT0 register when EOC interrupt pin is enabled. The obtained output from ADC is fed to the buffer for processing PQ information. The amount of DC inserted using a level translator of a signal conditioning circuit is eliminated by subtracting the same amount of digital DC value. The digital DC is obtained by subtracting analog DC with a number 2048 and scaling down to unity magnitude for further processing. The coefficients of high-pass, low-pass, and Hilbert filters are designed in MATLAB, and these coefficients are attached to the main program as a

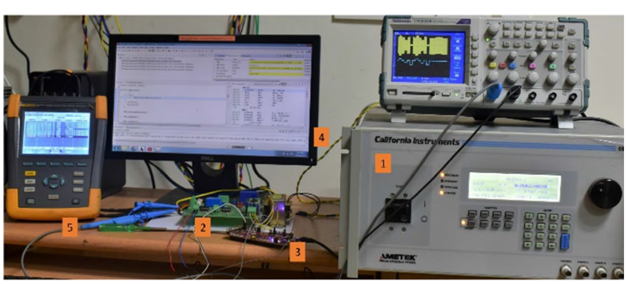

Fig. 2 Laboratory prototype of the developed hardware for real-time PQ monitoring with 1 is programmable power supply, 2 is signal conditioning circuit, 3 is TMS320F28379DL, 4 is PC running with code composer studio, 5 is fluke analyzer

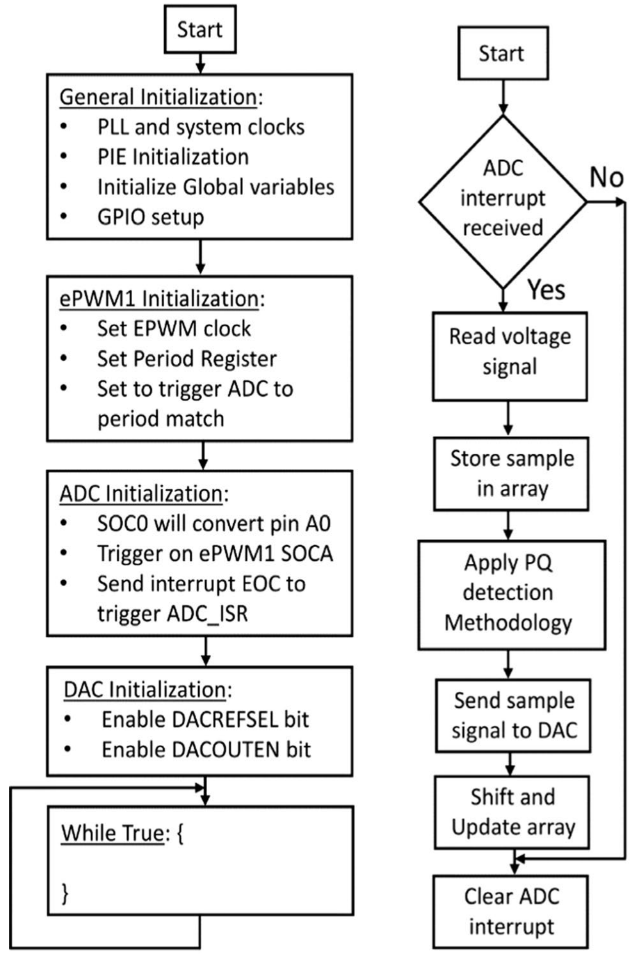

Fig. 3 Software implementation of the proposed algorithm on TMS320F28379D Launchpad

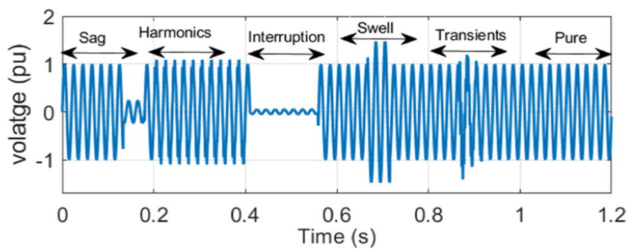

Fig. 4 PQ signal with sag, harmonics, interruption, swell, oscillatory transients, and normal events

header file to avoid the computational overhead for real-time processing. Finally, a 12-bit DAC unit is configured to produce the results in DO. The result of the proposed algorithm is copied into the DACVALS register of the DACb unit.

4 Results

This section presents the usefulness of the proposed algorithm for the detection and classification of synthetic PQ events of signals in a noisy and noise-free environment.

To detect and identify the events, the magnitude and time duration are considered for each of the signals. An example of the PQ disturbance signal is shown in Fig. 4. The signal consists of the following events such as sag, harmonics, interruption, swell, oscillatory transients, and normal PQ signal. The signal is decomposed into low-frequency and high-frequency components of the disturbance via the LPF and HPF. The LPF response consists of low-frequency information such as sag, swell, interruption, and normal signal, as shown in Fig. 5a. The envelope of the filtered signal is obtained from the HT, and its response is shown in Fig. 5b. Further, the MA filter is used to reduce ripples in the envelope, and its response is shown in Fig. 5c. Otherwise, these ripples can cause a false classification of the events when the envelope is near the decision boundaries of swell, sag, and interruption. The MA filter output is given to the derivative filter to represent the starting and ending points of the disturbance, as shown in Fig. 5d. Now, the responses of the MA filter and the derivative filter are given to the fuzzy classifier. Figure 5e shows the fuzzy classifier response for the given PQ signal. These events are indicated with numerical numbers: one represents the interruption, two represents the sag, three represents the normal, and four represents the swell.

Similarly, the high-frequency portion consists of harmonics, oscillatory events, and other events such as impulsive transients, phase jumps, and notches. The detection capability of the proposed PQD algorithm has been restricted to only harmonics and oscillatory transients by utilizing a simple time-duration feature. Figure 6a indicates the response of a high-pass filter. To nullify the phase jumps that occur

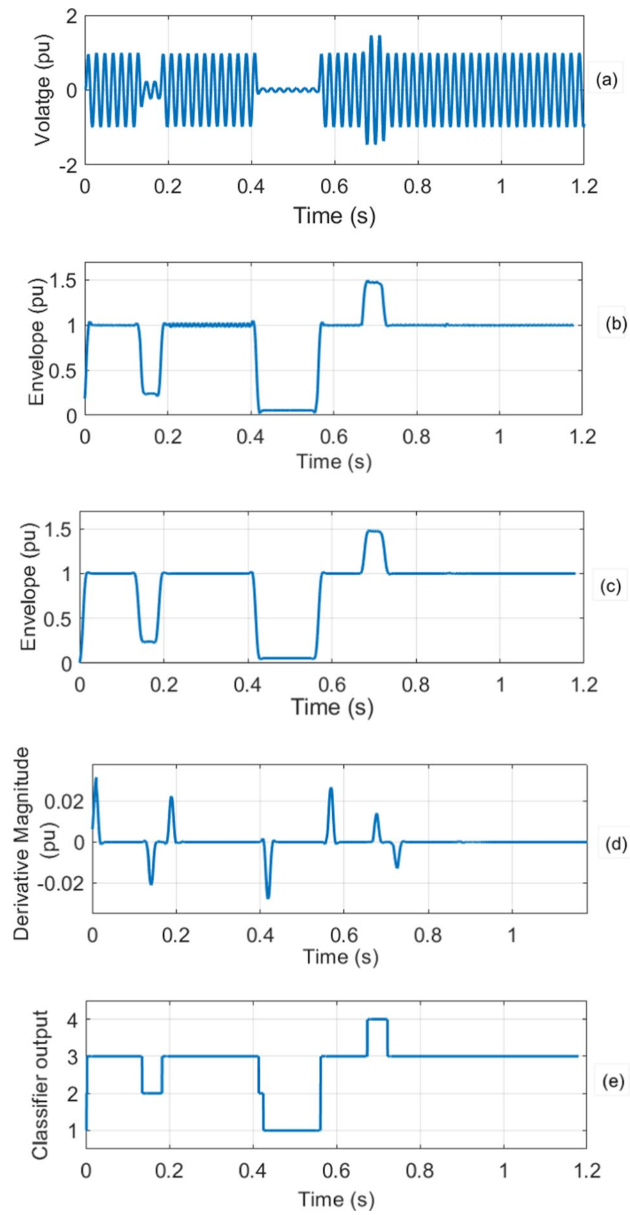

Fig. 5 Responses of different stages **a** low-pass filter **b** instantaneous amplitude **c** moving average filter **d** derivative filter e) fuzzy logic

due to the transitions of voltage variation events, the high pass filter output is given to a zero-mapping unit when the derivative filter magnitude is either greater than 0.001 or less than − 0.001. Figure 6b shows the zero-mapping unit response. It removes the phase jump response at different time instants, such as 0.13 s, 0.18 s, 0.41 s, 0.56 s, and 0.71 s. The output of the zero-mapping unit is given to HT to track the envelope of the PQ disturbance signal, as shown in Fig. 6c. To get a smooth envelope, the PQ signal is given to the MA filter, and its corresponding response is shown in Fig. 6d. This filter further reduces the phase jumps in the disturbance signal. The output of the MA filter is given to

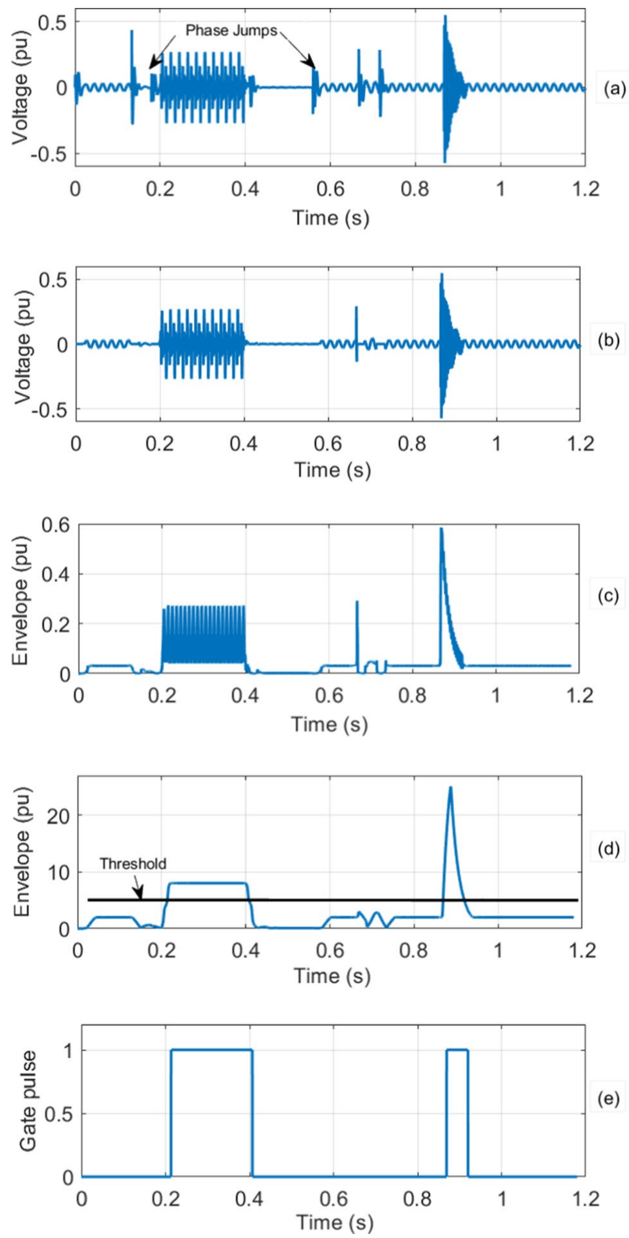

Fig. 6 Responses of different stages **a** highpass filter **b** zero-mapping unit **c** envelope **d** moving average filter **e** threshold unit

the threshold unit to detect the disturbance signal duration and its response shown in Fig. 6e. The harmonic and oscillatory transients are classified based on the signal duration.

4.1 Classification Accuracy of the Proposed Method

4.1.1 Synthetic Signals

Initially, these PQ signals are simulated in MATLAB using numerical models according to the IEEE 1159–1195 standard, as shown in Table 2. A total of 3000 disturbance signals are generated with the following specifications: sampling frequency of 3.2 kHz, 50 Hz fundamental frequency, and a 200 ms frame. Finally, these disturbances, such as sag, swell, interruption, normal, harmonics, and oscillatory events, are grouped into a single signal.

In order to verify the robustness of the proposed method, the additive white Gaussian noise is added to the disturbance signals with different SNR's of 40 dB, 30 dB, and 20 dB. The classification accuracy of the proposed method is summarized in Table 4. The results show that the proposed method provides promising outcome in the cases of noise-free environment, 40 dB, and 30 dB with an accuracy of 99.27%, 99.03%, and 98.70% respectively. The classification accuracy decreases as the noise magnitude increases. However, the proposed method achieves decent accuracy of 97.63% at a 20 dB SNR level. The accuracy of the proposed method is reduced majorly due to mis-classification of oscillatory transients, and the duration of these events exceeds the predefined levels in the noisy scenario. Similarly, in the case of sag and interruption, the accuracy is slightly reduced due to distortion in fuzzy classifier response at the boundaries of decision levels when noise levels increases. However, these distortions are limited to minimal by using the MA filter.

In order to show the effectiveness of the proposed method, the classification results are compared with the past studies reported in the literature, as shown in Table 5. It includes a comparison with the techniques of the Hilbert transform with radial basis function neural networks [23], Wavelet transform with support vector machine [24], Kalman filter with fuzzy logic [25], and Hilbert transform

Table 4 The classification accuracy of the proposed algorithm for PQ disturbance on synthetic signals

PQ disturbance signal	Correct classification rate			
	Clean signal	SNR = 40 (dB)	SNR = 30 (dB)	SNR = 20 (dB)
Normal	500	500	500	500
Sag	500	500	498	492
Swell	500	500	500	500
Interruption	500	499	497	483
Harmonics	500	500	500	500
Oscillatory transients	478	472	466	461
Average (%)	99.27	99.03	98.70	97.87

Table 5 Performance comparison of existing methods

Method	No of features	No of PQ events	Hardware setup	Accuracy
[23]	4	6	PC	94.00
[24]	10	5	PC	98.51
[25]	3	7	PC	98.71
[26]	5	9	PC	98.88
Proposed	4	6	PC	99.27

with feed-forward neural network [26]. Evaluation results show that the proposed method works better than other already reported methods. The proposed method is more capable of better classification since combining filtering techniques with the Hilbert transform can separate the sinusoidal and non-sinusoidal disturbances from the PQ signal.

4.1.2 Real-Time Signals

The experimental setup has been developed for real-time recognition of the disturbance present in a PQ signal. In order to validate the performance of the algorithm on real-time signals, 100 different types of each disturbance signal are considered for the analysis and tested successfully on a hardware platform. These signals are generated using a PPS as per the IEEE standard 1159–1195.

In this work, we have demonstrated results on the DSO, it consists of 0.5 s of swell, 0.5 s of sag, and 0.5 s of interruption in a pure signal denoted as V_S, as shown in Fig. 7a. The classifier response is collected from the DAC unit of TMS320F28379D Launchpad, which is denoted as V_d in Fig. 7a. We noticed that the method takes nearly 22 ms for detecting the normal, swell, sag, and interruption present in a PQ signal. Figure 7b, c shows harmonics and oscillatory transients detection on the DSO, and it provides a fixed delay of 25 ms for detecting these events. Table 6 shows the detailed step-by-step classification accuracy of each event on the TMS320F28379D Launchpad. It achieves an overall accuracy of 97.17% on the hardware platform. The sampling frequency has been set to 3.2 kHz. Therefore, the total time between samples is 312.5 μs and the average execution time for the detection and classification of events is 291 μs. The proposed method achieves the execution time without using optimization and it can be further reduced by using optimization. The proposed methodology has been compared with Fluke 435 in terms of measuring magnitude and duration of the events like sag, swell, and interruption, as shown in Table 7. However, the proposed approach can acquire the exact time duration of oscillatory transients and harmonics, which is an added advantage over the Fluke 435. Moreover, the proposed technique provides an accurate classification in case of an interruption event, whereas the Fluke 435 provides a Dip (sag).

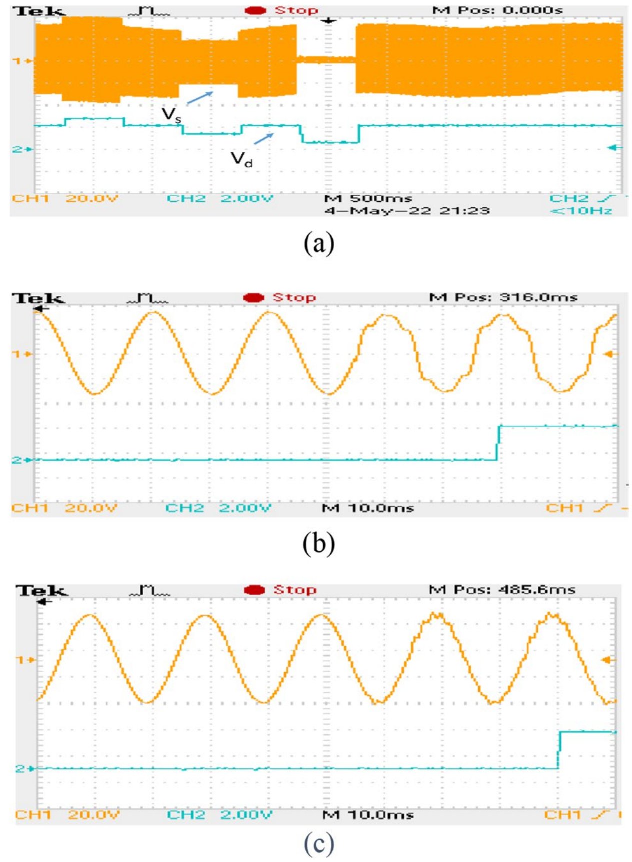

Fig. 7 Results of the proposed method on the experimental setup **a** Detection of sag, swell, normal, and interruption **b** Detection of harmonics **c** Detection of oscillatory transients

5 Discussion

In this work an automatic, real-time PQ event detection and classification algorithm with lower complexity is proposed. The method obtains the PQ information by sample-to-sample processing, unlike most of the methods that utilizes ten cycles information. This method utilizes Hilbert transform for envelope extraction. The simple features are extracted

Table 6 The classification results of the proposed method for PQ disturbance on experimental setup

PQ disturbance signal	Testing events	Recognized events	Recognized rate (%)
Normal	100	100	100.00
Sag	100	97	97.00
Swell	100	100	100.00
Interruption	100	96	96.00
Oscillatory transients	100	90	90.00
Harmonics	100	100	100.00

Table 7 Application test of proposed PQD device

PQ disturbance signal			Fluke 435			Proposed method		
True event	Magnitude (V)	Event duration (ms)	True event	Magnitude (V)	Event duration (ms)	True event	Magnitude (V)	Event duration (ms)
Int	17	500	Dip	14.2	508	Int	16.2	505
Sag	150	500	Dip	147.5	509	Sag	148	502
Swell	270	500	Swell	277.2	500	Swell	275	500

from the envelope and used for classification. The advantage of the proposed method is faster, and accurate in classification. The sample-to-sample processing time of the proposed algorithm is less than 291 μs. This helps in identifying the PQ events timely.

In [27], the authors proposed a CNN based PQ recognition algorithm for identifying nine power quality events. It achieves superior classification accuracy of 99.92%. However, it utilizes a window of 0.4 s for identifying disturbances, which is serious limitation for online mitigation of PQ events. In practical scenario, for implementing the CNN based algorithm requires high-end signal processing board. It is noteworthy to mention that monitoring of PQ events at various locations using this algorithm is not cost-effective solution. In [28], the authors presented on Hilbert Huang based detection and LSTM based classifier for power quality events recognition. The proposed method identifies the nine power quality events with a descent classification accuracy of 98.85%. However, this technique is not suitable for implementing due to the resource constraint, as it requires high performance computing devices.

It is important to notice that the objective of the proposed algorithm has been accomplished in terms of lower complexity, and usage of low-cost devices. Thus, this work is suitable for recording the power quality events with their corresponding magnitude and duration of the event. The superiority of the proposed algorithm is that, it need notrecord the PQ events continuously. Instead, it can record PQ events at the moment of event triggering. This work can be extended for online mitigation of PQ events such as sag, swell, harmonics and interruptions. Also, it can be applied to internet of things-based power quality event monitoring system by adding wireless communication protocols to the existing hardware setup. It helps in monitoring power quality events in remote locations.

The main limitation of the proposed algorithm is, it can only detect sag, swell, interruption, harmonics and oscillatory transients. However, the other events such as notches, flicker etc., are also present in the power system, but their frequency of occurrence is less.

6 Conclusion

This paper is presented on the design and development of an automatic real-time PQ monitoring for timely identification of PQD information. The PQD algorithm consists of Hilbert transform and fuzzy classifier for detection and identification of power quality events. The simple magnitude and duration features are extracted from the filtered signal. The proposed algorithm has been implemented on the TMS320F28379D Launchpad to show the real-time feasibility along with various simulation studies in MATLAB. Experimental results demonstrated that the proposed real-time PQ monitoring system can automatically detect and classify PQ events into normal, swell, sag, interruption, harmonics, and oscillatory transients with classification accuracy of 90–100%. The real-time implementation illustrates that the proposed PQ monitoring system can be integrated with smart metering for timely detection of PQ disturbances. In the future direction, the proposed PQD device can be unified with IoT- enabled smart metering applications.

Acknowledgements This work was financially supported by the Department of Science and Technology (DST), India and The European Union's Horizon 2020 Research and Innovation Program through the RE-EMPOWERED project under the Grant Agreement No DST/TMD/INDIA/EU/ILES/2020/50(c) and 101018420.

References

1. Bollen MH, Gu IY (2006) Signal processing of power quality disturbances. Wiley, Hoboken
2. IEEE Standard 1195: IEEE recommended practices for monitoring power quality, pp 1–59
3. Balwani MR, Thirumala K, Mohan V, Bu S, Thomas MS (2021) Development of a smart meter for power quality-based tariff implementation in a smart grid. Energies 14(19):6171
4. Alonso-Rosa M, Gil-de-Castro A, Medina-Gracia R, Moreno-Munoz A, Cañete-Carmona E (2018) Novel internet of things platform for in-building power quality submetering. Appl Sci 8(8):1320

5. Abbasi AR, Mahmoudi MR (2021) Application of statistical control charts to discriminate transformer winding defects. Elect Power Syst Res 191:106890
6. Abbasi AR, Mahmoudi MR, Arefi MM (2021) Transformer winding faults detection based on time series analysis. IEEE Trans Ins Measurement 70:1–10
7. Wright PS (1999) Short-time Fourier transforms and Wigner-Ville distributions applied to the calibration of power frequency harmonic analyzers. IEEE Trans Ins Measurement 48(2):475–478
8. Garcia CI, Grasso F, Luchetta A, Piccirilli MC, Paolucci L, Talluri G (2020) A comparison of power quality disturbance detection and classification methods using CNN LSTM and CNN-LSTM. Appl Sci 10(19):6755
9. Moravej Z, Abdoos AA, Pazoki MJEPC (2009) Detection and classification of power quality disturbances using wavelet transform and support vector machines. Elect Power Comp Syst 38(2):182–196
10. Masoum MAS, Jamali S, Ghaffarzadeh N (2010) Detection and classification of power quality disturbances using discrete wavelet transform and wavelet networks. IET Sci Measurement Tech 4(4):193–205
11. Deokar SA, Waghmare LM (2014) Integrated DWT–FFT approach for detection and classification of power quality disturbances. Int J Elect Power Energy Syst 61:594–605
12. Kumar R, Singh B, Shahani DT, Chandra A, Al-Haddad K (2014) Recognition of power-quality disturbances using S-transform-based ANN classifier and rule-based decision tree. IEEE Trans Ind Appl 51(2):1249–1258
13. Amirou A, Amirou Y, Ould-Abdeslam D (2022) S-transform with a compact support kernel and classification models based power quality recognition. J Elect Eng Tech 17:1–10
14. Samanta IS, Rout PK, Mishra S (2020) Power quality events recognition using s-transform and wild goat optimization-based extreme learning machine. Arab J Sci Eng 45(3):1855–1870
15. Camarena-Martinez D, Valtierra RM, Perez-Ramirez CA, Amezquita-Sanchez JP, de Jesus-Romero-Troncoso R, Garcia-Perez A (2015) Novel down sampling empirical mode decomposition approach for power quality analysis. IEEE Trans Ind Elect 63(4):2369–2378
16. Liu Z, Cui Y, Li W (2015) A classification method for complex power quality disturbances using EEMD and rank wavelet SVM. IEEE Trans Smart Grid 6(4):1678–1685
17. Sahani M, Dash PK (2018) Automatic power quality events recognition based on Hilbert Huang transform and weighted bidirectional extreme learning machine. IEEE Trans Ind Inf 14(9):3849–3858
18. Behzadi M, Askari MT, Amirahmadi M, Babaeinik M (2022) Dual identification of multi-complex and non-stationary power quality disturbances using variational mode decomposition in hybrid modern power systems. Arab J Sci Eng 20:1–21
19. Arif A, Al-Hussain M, Al-Mutairi N, Al-Ammar E, Khan Y, Malik N (2013) Experimental study and design of smart energy meter for the smart grid. In: 2013 International renewable and sustainable energy conference (IRSEC), IEEE pp 515–520
20. Capriglione D, Ferrigno L, Paciello V, Pietrosanto A, Vaccaro A (2016) Experimental characterization of consensus protocol for decentralized smart grid metering. Measurement 77:292–306
21. Achlerkar PD, Samantaray SR, Manikandan MS (2016) Variational mode decomposition and decision tree based detection and classification of power quality disturbances in grid-connected distributed generation system. IEEE Trans Smart Grid 9(4):3122–3132
22. Parvez I, Aghili M, Sarwat AI, Rahman S, Alam F (2019) Online power quality disturbance detection by support vector machine in smart meter. J Modern Power Syst Clean Energy 7(5):1328–1339
23. Jayasree T, Devaraj D, Sukanesh R (2010) Power quality disturbance classification using Hilbert transform and RBF networks. Neurocomputing 73(7–9):1451–1456
24. Eristi H, Demir Y (2012) Automatic classification of power quality events and disturbances using wavelet transform and support vector machines. IET Gener Trans Distrib 6(10):968–976
25. Abdelsalam AA, Eldesouky AA, Sallam AA (2012) Characterization of power quality disturbances using hybrid technique of linear Kalman filter and fuzzy-expert system. Elect Power Syst Res 83(1):41–50
26. Granados-Lieberman D, ValtierraRodriguez M, Morales-Hernandez LA, Romero-Troncoso RJ, Osornio-Rios RA (2013) A hilbert transform-based smart sensor for detection, classification, and quantification of power quality disturbances. Sensors 13(5):5507–5527
27. Topaloglu I (2022) Deep learning based a new approach for power quality disturbances classification in power transmission system. J Elect Eng Tech 11:1–12
28. Rodriguez MA, Sotomonte JF, Cifuentes J, Bueno-L'opez M (2021) A classification method for power-quality disturbances using Hilbert–Huang transform and LSTM recurrent neural networks. J Elect Eng Tech 16(1):249–266

Naveen Kumar Buduru received his B.Tech. degree in electronic and communication engineering from JNTUACE, Pulivendula, India, in 2011, the M.Tech. degree in digital signal processing from IIST, Trivandrum, India, in 2016. He is currently pursuing Ph.D. degree in school of electrical sciences at the IIT Bhubaneswar, Bhubaneswar, India. He is currently conducting research in design and development of IoT based power quality monitoring system. His research interests include signal processing for power quality, and Internet of Things.

Srinivas Bhaskar Karanki received his B.Tech. degree from the Acharya Nagarjuna University, Guntur, India, in 2007, and the Ph.D. degree in electrical engineering from the Indian Institute of Technology Madras, Chennai, India, in 2012. From 2012 to 2014, he was a Post-Doctoral Fellow in Centre for Urban Energy (CUE), Ryerson University, and Toronto, Canada. He is currently an Assistant Professor in the School of Electrical Sciences, IIT Bhubaneswar, Bhubaneswar, India. His current research interests include power electronic converters for renewable energy systems, power quality, energy storage, and power electronics applications in power systems.